ECOPERSIA

DOI: 10.18869/modares.Ecopersia.5.2.1771 **2017, 5 (2): 1771-1786**

Digital Mapping of Topsoil Salinity Using Remote Sensing Indices in Agh-Ghala Plain, Iran

Seyedeh Zohreh Mousavi[1*], Mahmood Habibnejad[2], Ataollah Kavian[3], Karim Solaimani[2], Farhad Khormali[4]

[1] *Ph.D Student of Watershed Engineering, Faculty of Natural Resources, Sari University of Agricultural Science and Natural Resources, Sari, Iran*

[2] *Professor of Watershed Engineering, Faculty of Natural Resources, Sari University of Agricultural Science and Natural Resources, Sari, Iran*

[3] *Associate Professor of Watershed Engineering, Faculty of Natural Resources, Sari University of Agricultural Science and Natural Resources, Sari, Iran*

[4] *Professor of Pedology, Faculty of Water and Soil Engineering, Gorgan University of Agricultural Science and Natural Resources, Gorgan, Iran*

**Corresponding author: Ph.D Student, Faculty of Natural Resources, Sari University of Agricultural Science and Natural Resources, Sari, Iran, Tell: +98 323 38291, Fax:+98 4235 2500, Email: zmousavi2006@gmail.com*

Received: 4 November 2016 / Accepted: 10 March 2017 / Published Online: 20 March 2017

Background: Soil salinization is a world-wide land degradation process in arid and semi-arid regions that leads to sever economic and social consequences.

Materials and Methods: We analyzed soil salinity by two statistical linear (multiple linear regression) and non-linear (artificial neural network) models using Landsat OLI data in Agh-Ghala plain located in north east of Iran. In situ soil electrical conductivity (EC) of 156 topsoil samples (depth of 0-15cm) was also determined. A Pearson correlation between 26 spectral indices derived from Landsat OLI data and in situ measured ECs was used to apply efficient indices in assessing soil salinity. The best correlated indices such as blue, green and red bands, intensity indices (Int1, Int2), soil salinity indices (Si1, Si2, Si3, Si11, Aster-Si), vegetation Indices (NDVI, DVI, RVI, SAVI), greenness and wetness indices were used to develop two models.

Results: Comparison between two estimation models showed that the performance of ANN model (R^2=0.964 and RMSE=2.237) was more reliable than that of MLR model (R^2=0.506 and RMSE=9.674) in monitoring and predicting soil salinity. Out of the total area, 66% and 55.8% was identified as non-saline, slightly and very slightly saline for ANN and MLR models, respectively.

Conclusions: This shows that remote sensing data can be effectively used to model and map spatial variations of soil salinity.

Keywords: Artificial neural network, Electrical conductivity, Landsat OLI data, Multiple Linear Regression, Iran

1. Background

Soil salinization is a term that includes saline, sodic and alkaline soils in arid and semi-arid regions that leads to severe economic and social consequences (17). Soil salinization is a widespread phenomenon, with saline and sodic soils covering 932.2 M ha globally (48), from which 34.19 Mha or over 10% of the total

irrigated land (5) are affected by soil salinization due to mismanaged irrigation. Global soil salinization hotspots include Pakistan, China, United States, India, Argentina, Sudan and many countries in Central and Western Asia (5, 24). With a climate predominated by little rainfall and adverse evapotranspiration rates, and soil characteristics that restrain salt leaching, arid irrigated lands are prominent salinization hotspots (17). Widespread extent of irrigated lands in central and northeast of Iran are affected by primary and secondary salinization. Land degradation, productivity loss and increasing the salt concentration lead to other soil degradation problems such as soil dispersion, sealing and compaction. This process is a serious problem that now is threatening sustainable agriculture and land management throughout the world. Therefore, early-stage identification and assessment of the extent and degree of severity of salinization are vital for sustainable land-use planning (42).

During the last two decades, remote sensing technology by using avariety of data, such as aerial photography, video images, infrared thermography, visible and infrared multispectral, and microwave images (8, 32) has been used widely for detecting soil salinity due to its wide spatial coverage, ability to update quickly, and low cost (21, 41). Among them, board band remote sensing data with various spatial and temporal resolution (Landsat TM - Landsat ETM - Spot XS – Ikonos – QuickBird- Aster ad IRS) have been generally used for monitoring salt affected soils (19, 36, 1,44). Despite some difficulties using multispectral sensors, such as their low spectral resolution and the use of conventional classification methods, including supervised classification and visual interpretation (53), they have been successful in differentiating between sever saline and non-saline soils(21, 50). Nevertheless, in recent years soil salinity mapping using multispectral images has progressed from qualitative approaches, such as classifying different degrees of salt affected soils (34, 21, 11), to quantitative digital mapping (44, 13, 26). Some more popular statistical techniques that have been frequently used in literatures are to map and identify relationships between soil properties, water, climate, topography, vegetation and salt parameters(e.g. EC or SSC) using linear regression model (MLR) (48,42,26) and artificial neural network (ANN) (22, 48, 2, 45).

2. Objective

Covering farmlands with great potential for agricultural development, Agh-Ghala plain is severely affected with salinization that poses the highest threat for agriculture (46). Therefore, detailed survey on the spatial variation of soil salinization is necessary to prevent further salinization and manage saline soil in this region. Several researchers have attempted to estimate and map soil salinization using reflectance composition indices obtained from Landsat TM or ETM+ images (44,13, 6). Nostudyon soil salinity estimation using Landsat 8 - OLI images has been recorded in Iran and studies in other parts of the world are very limited (26). Therefore, we attempted to investigate soil salinity variation using spectral indices derived from Landsat 8 OLI data through two quantitative models for an area within Iran. Therefore, the main objectives of this study were: 1) to identify and analyze the relationship between spectral indices of Landsat 8 (OLI) and topsoil salinity (through EC) in depth of 0-15 cm in parts of Agh-Ghala plain of Iran, and whether spectral indices were effective on soil salinity estimation, and 2) Digital mapping and to estimate soil salinity using remote sensed images and two statistical predictive models (MLR and ANN) and analyzing the better method by comparing their estimation accuracy.

3. MATERIALS AND METHODS

3.1. Study area

The study site (Figure1c) lies in north-east of Agh-Ghala plain in Golestan Province that covers an area of 3500 h (37˚ 41' 9" to 37˚ 7'8" N and 54˚ 28' 26" to 54˚ 35' 52"E). The highest elevation is about 47.4 m in eastern side and the lowest one is about 30.9 min southwest side of the study area. Climate of the area is mild and semi-arid with the mean annual temperature of 18.8 ˚C. The mean annual precipitation is approximately 367.5 mm, most of which is received between June and September. The mean annual evapotranspiration is 1073.643 mm, almost 3 times the mean annual precipitation.

The most common land use of the region is farmland that is mostly under wheat, rapeseed and barley and in summer they are generally under fallow and secondary cultivation of rice, sunflower and cotton. Morphologically, the region includes river alluvial plain type whose parent materials are alluvial. Dominated soil texture of the area is silty-clay that is suitable for agriculture but poses some difficulties in sustainable agriculture due to high amounts of salt and sodium in top soil texture. Because of higher level of the ground water table (mostly at a depth of 1-2 m) and rise back of salts in the drained water by capillary rise, soil surface salinization is happening in the area (43).

3.2. Soil sampling

Initially, the corners of a network with 500 meter intervals in the study area were designated as location of soil sampling, but due to some natural and morphological conditions as well as different land uses in the study area, some sample locations were modified (Figure1c). In July 2014, 156 soil samples were collected from top soils (0 to 15 cm) of the designated locations, and upon drying, their EC were measured in laboratory in their saturated paste extract (30).

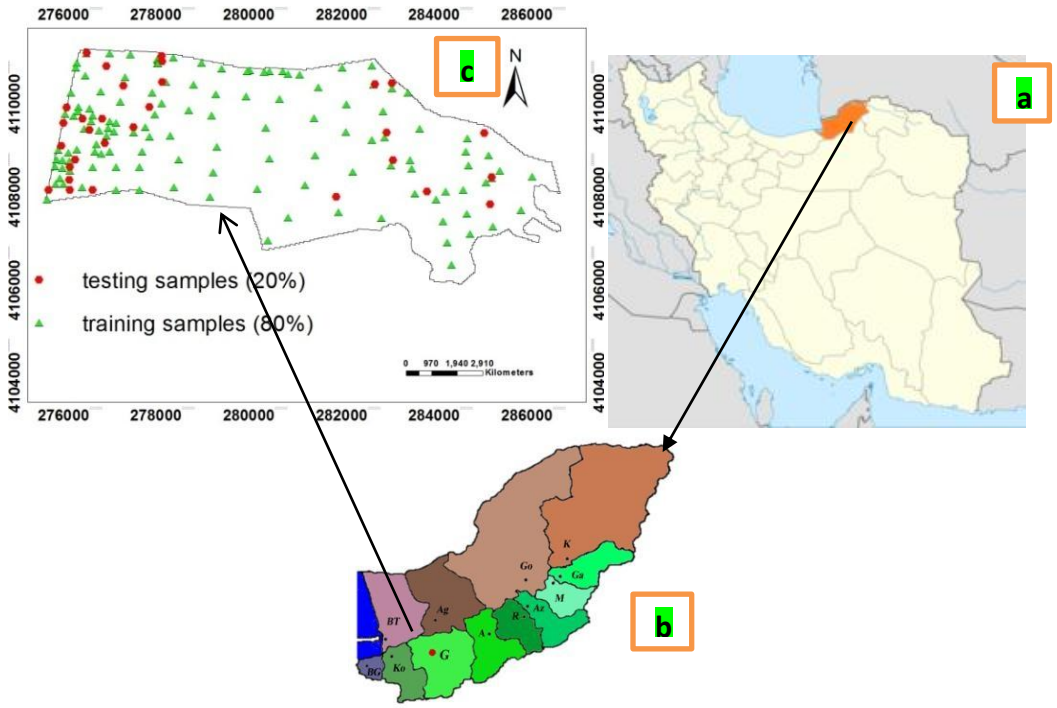

Figure 1 Location of the study area and spatial pattern of soil sampling points

3.3. Landsat data preprocessing

The multispectral Landsat 8 (OLI- TIRS) satellite image (path 163-row 34) was acquired on July 10, 2014. The Landsat 8 carries two instruments: (1) the Operational Land Imager (OLI) that collects image data for nine shortwave spectral bands (OLI1~ OLI9) over a 185 km swath with a 30 m spatial resolution for all bands except a 15 m panchromatic band (OLI8), (2) the thermal infrared sensor (TIRS) that collects image data for two thermal bands (TIRS10, TIRS11) with a 100 m resolution over a 185 km swath (29). The Landsat 8 (OLI-TIRS) data was geometrically corrected using a corrected image to exactly geolocate the sample point locations and also clearly show the surface reflectance of the soil samples. Nevertheless, atmospheric correction was performed on land sat 8 (OLI-TIRS) data based on dark subtract method using ENVI 4.5 software to match the image data to the real surface reflectance spectra.

3.4. Remote sensing indices and processing

According to several spectral combinations highlighted in the literatures, as the primary input, 26 spectral indices and bands used that were generated from four different remote sensing indicators, viz. salinity, intensity, vegetation and spectral indices and bands from (OLI) sensor of Landsat 8 (Table 1).

Table 1 Applied salinity effective indices and bands of Landsat8 on the study area

	Indices		
Salinity indices	Sl1	$\sqrt{B3 \times B4}$	(1)
	Sl2	$\sqrt{B3^2 + B4^2 + B5^2}$	(2)
	Sl3	$\sqrt{B3^2 + B4^2}$	(4)
	Sl-11	B5/B6	(5)
	Aster_Sl	(B5-B6)/(B5+B6)	(6)
Intensity indices	Int1	(B3+B4)/2	(7)
	Int 2	(B3+B4+B5)/2	(8)
	BI	$\sqrt{B3^2 + B5^2}$	(9)
	SAVI	(B5-B4) × (1+L) / (B5+B4+L)	(10)
Vegetation indices	NDVI	(B5-B4) / (B5+B4)	(11)
	DVI	(B5-B4)	(12)
	WDVI	B5-(a ×B4)	(13)
	PVI	$\frac{NIR-(a.R+b)}{\sqrt{1+a^2}}$	(14)
	TSAVI	$\frac{NIR-(a.R+b)}{R+A.(NIR-b)+0.08(1+a^2)}$	(15)
Spectral Indices	B2-B3-B4-B5-B6-B7		
	COSRI	(B2+B3) / (B4+B5) × NDVI	(16)
	MSI	B6/B5	(17)
	Brightness	0.3037×B2+0.2793×B3+0.4743×B4 +0.5585×B5+0.5082×B6+0.1868×B7	(18)
	Greenness	-0.2848×B2-0.2435×B3-0.5436×B4+0.7243×B5+0.0840×B6-0.1800×B7	(19)
	Wetness	0.1509×B2+0.1973×B3+0.3279×B4-0.3406B5-0.7112×B6-0.4572×B7	(20)

B2, B3, B4, B5: blue, green, red, near-infrared bands, B6 and B7: infrared bands of Landsat8 image; bands of Landsat8 image respectively; a, b: soil line coefficients. L: a constant equals to 0.5; Int1 and 2: intensity within the visible spectral range and VIS-NIR spectral range respectively (19); BI: brightness index (31); NDVI: normalized difference vegetation index (40); SAVI: soil-adjusted vegetation index (28); DVI: difference vegetation index (14); WDVI: weighted difference vegetation index (14); PVI: perpendicular vegetation index (49); TSAVI: transformed soil-adapted vegetation index (7); COSRI: Combined Spectral Response Index (23); Brightness, Greenness and Wetness (33).

A Pearson correlation between 26 remote sensing data and EC measurements was made to identify the efficiency of each index in assessing soil salinity and omit non-correlated parameters with ECs. Furthermore, a single correlation analysis between independent variables shows that there is high correlation between them. Spectral bands and indices involve many variables and they tend to be of high multicollinearity (42) that specially is worse in constructing linear statistical models. Therefore, other non-linear methods are required to eliminate redundant information of variables. All the statistical operations were done using SPSS (version 22).

3.5. Spatial prediction models of EC

3.5.1. MLR

Multiple linear regressions (MLR) is a multivariate statistical technique that assesses the coefficients of the linear equation, using two or more independent variables to predict the dependent variable. After selecting spectral indices correlated with in situ ECs (as predictor variables), 80% of the soil samples areselected to calibrate the model and the remaining 20% to validate the model prediction based on T-Test (47). According toTomasella *et al*. (47), if there is no significant difference between means and standard deviations of two data sets, better results can be expected from statistical models. Several multiple linear regressions (MLR's) are explored in this study to predict soil salinity.

The choice of the best model is based on the coefficient of multiple determination (R^2) computed by the model (20, 51, 10). Remained indices in the best model show the highest correlation with the EC from the ground truth (10).The resulting model was used to estimate the image-scale soil ECand to map the distribution of soil salinity. All statistical operations and making soil salinity map were done using SPSS (version22), Idrisi (Selva) and ARC GIS (10) software, respectively.

3.5.2. Artificial neural network model (ANN)

Artificial neural network is a mathematical model that has the ability to place the non-linearity processes in order to set relationship between input and outputs in any systems. The neural network includes three layers, viz. input, output, and hidden layers, within which there are nods or nerve cells (neurons) connected to the next neurons through the weights. In this study, a multiple –layer feed–forward back propagation network with three layers was used: an input layer with 16 neurons including remote sensing data representation of independent variables (blue, red and green bands, Si1, Si2, Si3,Si11,Aster Si, Int1,Int 2, NDVI, DVI, RVI, SAVI, wetness and greenness Indices), a hidden layer and an output layer. Tan-sigmoid transfer function (non-linear) has been used in hidden layer so as to allow only approximate non-linear relations (to) present between input and output layers (27). The Levenberg-Marguardt algorithm was used for network training because of its efficiency, simplicity and fast optimization (4).The number of neurons in hidden layer, in the present study were varied from 16 to 25 and the most appropriate number was decided by a trial- and-error method (12) in order to minimize error criterions of the model. Data preprocessing

technique of standardizing to a mean of zero and standard deviation of one were applied to the inputs to normalize the remote sensing data according to bellow equation:

$$X_{istd} = \frac{X_i - X_{i\min}}{X_{i\max} - M_{i\min}} \quad (21)$$

Where X_{istd} is the standardized value of variable, X_i is the original value and X_{imax} and X_{imin} are the maximum and minimum of variable respectively.

For model calibration and validation, all sample points of EC measurements were divided into two subsets, one for training the network (80% of input data) and another for testing the network performance (20%) as mentioned in 2.3.1. section. For ANN modeling, the computer software Matlab (2011) and the neural network tool box were used (18).Digital mapping of soil salinity of the study area based on final weights of the most appropriate neural network in terms of size and performance was made in ARC GIS software (version10).

3.6. Cross validation of top statistical models

To compare the performance and sufficiency of MLR and ANN prediction models for soil salinity, four different criteria, viz. root mean square error (RMSE), RSE (Relative standard Error), R^2 (coefficient of determination, and ME (mean error) for the estimated EC values (Y') and measured EC in field were calculated (equations 22-25).

$$RMSE = \sqrt{\frac{1}{n}\sum_{i=1}^{n}(Zo - Zp)^2} \quad (22)$$

$$RSE = \frac{\sqrt{\frac{1}{n}\sum_{i=1}^{n}(Zo - Zp)^2}}{Zo_{ave}} \quad (23)$$

$$ME = \frac{1}{n}\sum_{i=1}^{n}(Zo - Zp) \quad (24)$$

$$R^2 = \left[\frac{\sum_{i=1}^{n}(Zo - Zo_{ave})(Zp - Zp_{ave})}{\sqrt{\sum_{i=1}^{n}(Zo - Zo_{ave})^2 (Zp - Zp_{ave})^2}}\right] \quad (25)$$

Where Zp denotes the predicted values, Zo is the observed value. Zo_{ave} and Zp_{ave} show the average of observed and predicted values, respectively, n is the number of data.

4. Results and Discussion

4.1. Descriptive statistics of EC data

The descriptive statistical analysis of soil salinity (Table2) showed that the EC of 156 samples ranged from 0.358 (dS m^{-1}) to 58.100 (dSm^{-1}) with the coefficient of variation (CV) of 1.25 (dS m^{-1}). It means that salinity in the study area was highly variable (52). The mean EC value of 9.896 indicated that half of soil samples were moderately salt affected. However, according to Table 3, the amount of non-saline, slightly and very slightly saline soil samples (EC<8 dSm^{-1}, 66% of all soil samples) were not only more than moderately and strongly saline soil samples (EC>8 dS m^{-1}, 33.98% of all samples) but also more distributed than them.

Table 2 Descriptive statistics of surface soil EC measurements

Layer (Cm)	Min	Max	Average	Std.deviation	CV (%)	Kurtosis	Skewness
EC (0-15cm) (dS m^{-1})	0.385	58.10	9.896	12.423	125.4%	2.378	1.721

4.2. Remote sensing processing

The Pearson correlation at a level of $p<0.05$ (2-tailed) was conducted between the measured ECs and Landsat OLI spectral bands and derived indices to reveal the more causative parameters on soil salinity, among which 17 predictor variables were significantly correlated with the measured ECs (Figure 3). Intensity, salinity and vegetation indices showed low correlation with the EC, varying from 0.211 to 0.297, 0.158 to 0.304 and -0.169 to -0.238, respectively. In terms of spectral bands and indices, moderate correlation belongs to B2 (0.419) that is the highest of them. According to Figure 3, because of low correlation between spectral bands and EC (upto 42%), the indices derived from them have alimited potential for detecting soil salinity. The low spatial resolution (30×30m) of the Landsat OLI data is one reason of such a weak correlation. Furthermore, remote sensing data cannot alone present perfectly all salinity characteristics of soils. The third reason is that limited collected samples cannot be completely representative of all pixels because one sample represents only one point on the relevant 30 × 30m pixel.

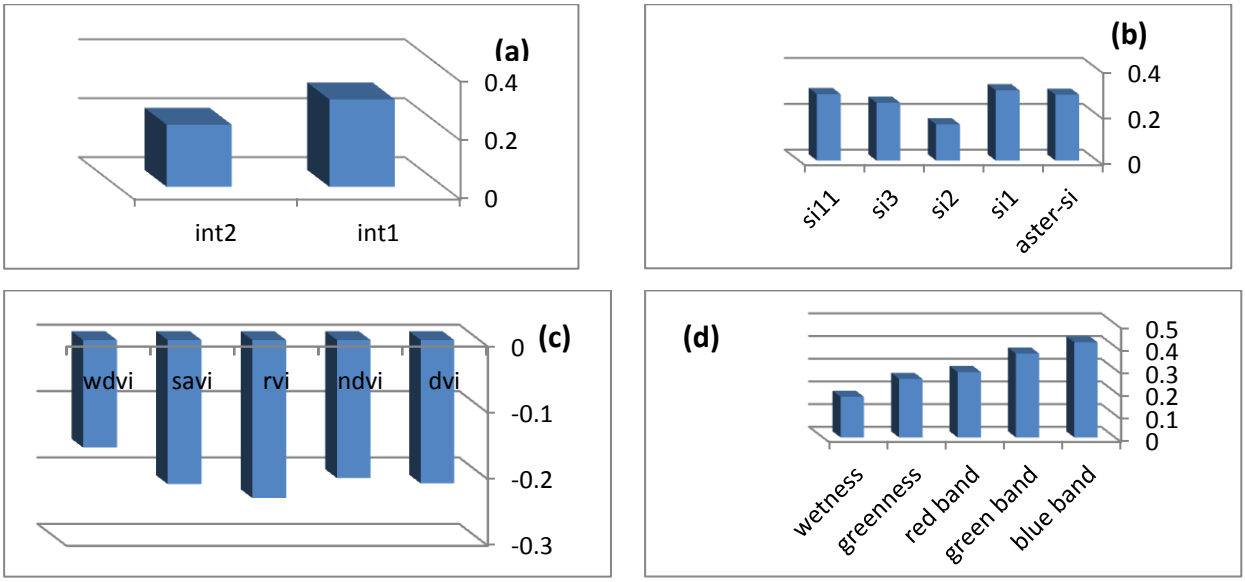

Figure 3 Correlation coefficients (y axis) between the measured ECs and indices, including intensity (a), salinity (b), vegetation (c), spectral bands and indices (d)

4.3. Statistical analysis

4.3.1. MLR

The MLR model as a linear statistical equation was used to estimate soil salinity of the region. From 17 parameters correlated with the measured ECs (Figure 3a-d), WDVI index was not significantly correlated with training ECs (80% of all ECs) and was omitted.The remaining indices were applied as predictor variables to build up MLR model. Among several explored models, the best one was found (equation 26) based on the coefficient of multiple determination (R^2). Combining these salinity indices helps to build a more reliable MLR empirical relationship to predict soil salinity. The regression relationship is given by following Equation:

Predicted (EC) = 36.889+0.024B2-160.142Aster-Si -60.676 RVI+0.005 wetness (26)

The best R^2 value in the regression output indicates that only 50% of the total variation of the predicted EC values can be interpreted by the predictor variables used in the model. The regression coefficients of the model showed that the Aster –Si contribution to the estimation of soil salinity had the highest value, followed by RVI index, blue band, and wetness index made the lowest contribution to the estimated soil salinity. The results of this research were slightly different from the earlier findings either in the contribution of the blue band (37, 42) or the spectral reflectance of the wetness index (45). These differences were most likely caused by differences in the study area, the chemical components of the soil, and the band range of the multispectral data as well as other possible factors. Four criteria, viz. RMSE, RSE and ME values were computed for evaluating the performance of two models for both prediction and validation data sets, having values of 9.331, 0.840 and 1.183, respectively, in the calibration process and 10.998, 1.733 and -0.789, respectively, in the validation process (Table 4). These results indicated that the accuracy of MLR model performance was reliable to assess spatial soil salinity. According to Table 4, the coefficient of determination (R^2) calculated for the best model equaled 0.5which was lower than the earlier findings of about 0.7 and 0.8 (13, 45).It reveals that soil salinity (EC) is not only influenced by remote sensing indices but also some other important terrain indices. Another reason is that the spectral reflectance of Landsat OLI data is influenced by moisture content and vegetation cover. So, several researchers have achieved good performance with linier regression models (6, 36, 3) due to the enhanced image efficiency in highlighting information from soil salinity and suppressing other details such as vegetation. Distribution map of the estimated EC into 6 classes using MLR model is shown in Figure 5, the definition of which is based on the visual interpretations combined with various levels of soil EC. These categories are: (1) non-saline soils, (2) very slightly saline soils, (3) slightly saline soils, (4) moderately soils, (5) highly saline soils and (6) severely saline soils.

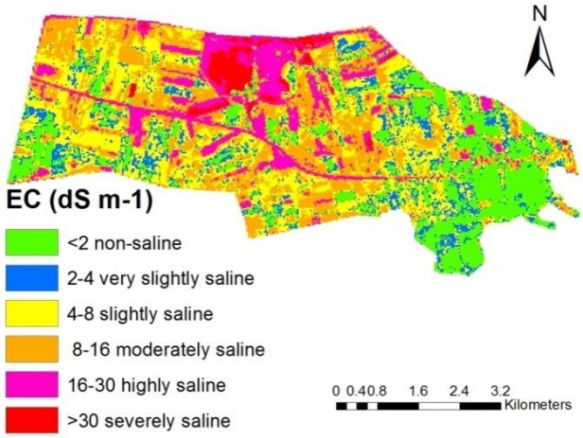

Figure 4 Predicted map of EC (dS m^{-1}) using MLR model

4.3.2. ANN

We used artificial neural network model to monitor and predict the soil salinity in terms of EC. After normalization of all the measured EC, a total of 126 points (80% of all EC point data) was used for calibration of the model, while the remaining data (20% of EC points) were used for validation. Using a trial- and- error method, 10 various network architecture with fixed 16 neurons and 1 in input and one output layers and different number of neurons (16 to 25) in hidden layer were schematized and among them the neural network schemed at 10-22-1 architecture, with the lowest RMSE error (2.371) and the highest R^2 (0.964), was selected as the most appropriate ANN architecture to predict and map spatial distribution of soil salinity (EC). Validation results for the ANN prediction model based on the training (80% of all data) and

validation data set (20% of all data) is presented in Table 4. The predictive accuracy of ANN model reached a high level (R^2=0.964 and RMSE= 2.371), indicating the measured and predicted values of ECs were highly correlated. So, ANN predictive modelhada great potential for estimating and mapping soil salinity, which was in agreement with the earlier works (22, 48) that confirmed the efficiency of ANN empirical method to predict soil salinity.

Soil salinity map within 6 classes of predicted EC using ANN method is shown in Figure 5.The extent of areas of each class of two salinity maps (MLR and ANN methods) is shown in Table4. ANN prediction model had predicted 66% of the total area as non-saline, slightly and very slightly saline classes, whereas the prediction was 55.8% in MLR model. Both prediction models could clearly identify the non-saline, slightly and very slightly saline soils were distributed in fallow and croplands covered by lacustrine sediments and shallow ground water level; severely saline soils were distributed in limited areas of saltmarshes in the northern part and other uncultivable or sparsely vegetated saline soil of the study area were covered with a thick layer of salt. Comparison of two salinity maps and land use classification map (Figure 6)revealed that in parts of the study area with concentrated cropland of summer crops (rice, cotton, sunflower), non-saline to slightly saline soils (0<EC<8 dS m^{-1}) were more distributed due to soil texture and proximity to irrigation canals and drainage network. According to Akhtar *et al.* (1), cropland class had more uniform canopy cover in winter cropping season due to widely grown wheat crop compared with summer cropping season. This is because of post-harvest fallow land previously under winter cropping (e.g. cereals), early growth stage of summer crops, and likely lack of natural vegetation's caused by hot and dry summer season.

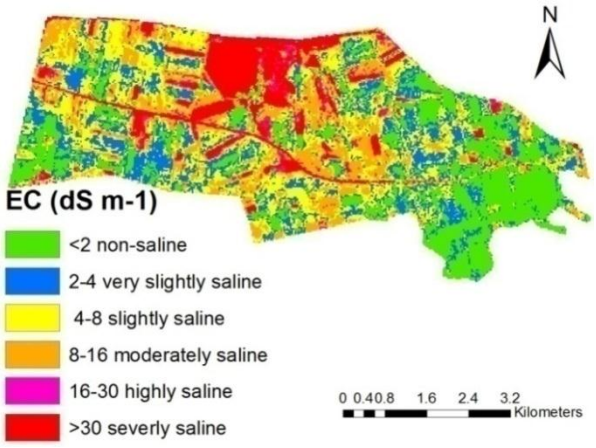

Figure 5 Predicted map of EC (dS m^{-1}) using ANN method

Table 3 Area extent of soil salinity level derived from MLR and ANN prediction models

Salinity Extent	EC value	Observed soil samples (n)	Observed soil samples (%)	Predicted area (ha) (MLR)	Predictedarea (%) (MLR)	Predicted area(ha) (ANN)	Predicted area (ha) (ANN)
Non-saline	0-2	51	32.69	633.69	19.3	789.75	24
Very slightly saline	2-4	27	17.30	344.25	10.5	619.74	18.9
Slightly saline	4-8	25	16.03	852.66	26	758.88	23.1
Moderately saline	8-16	19	12.18	921.69	28.1	631.53	19.23
Highly saline	16-30	19	12.18	427.59	13	130.32	4
Severely saline	>30	15	9.62	104.58	3.1	354.24	10.8
Total		156	100	3284.46	100	3284.46	100

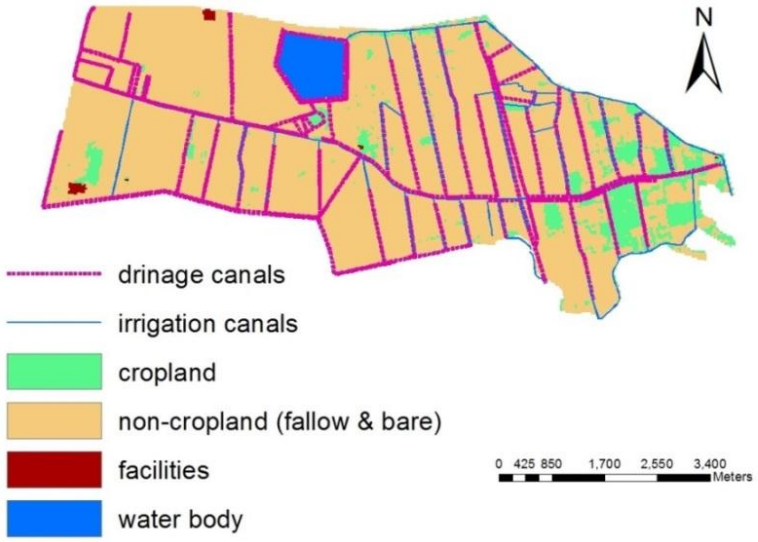

Figure 6 land-use classification map

With regard to the soil salinity maps (Figures 5 and 7), highly saline and severely saline soils belonged to the northern part of the region. This is considerable because of lack of irrigation canals and deficient drainage network in northwest of the study area (Figure 6). Additionally, dried out water body in north with a thin surface salt all across it as well as being a stripe of salt flat exactly on north of the water body are more than explanations of the problem. This is reasonable to overcome soil salinity complications in future by reforming incomplete irrigation and drainage canals and feeding the water body by river, through irrigation canals in the study area.

4.4. Validation and comparison of two models

A predictive statistical model based on MIR analysis with 16 independent variables and the measured EC points was constructed to compare it with ANN predictive model and evaluate the latter's reliability. The results indicated that the ANN prediction model hada greater accuracy than the MLR model. The R^2 value of the ANN predictive model was 0.964, while the R^2 of the MLR model was 0.506. The RMSE and ME values were 2.371 and -0.059 for ANN model that were lower than RMSE and ME values of 9.674 and 0.804, respectively, for MLR predictive model (Table 5). A single correlation analysis between 16 predictor variables showed that there were high correlations between them with the range of 16.1% to 99.5% that made multicollinearity between independent variables and caused to some extent less reliable predicted values of EC in linear regressions. Therefore, the ANN method was more suitable than MLR model to estimate soil salinity, which was in agreement an earlier study (45) in which both feed forward ANN (R^2=0.68, RMSE= 36.67) and cascade forward ANN (R^2= 0.68, RMSE= 38.10) had more reliable performance than MLR method. (R^2= 0.66, RMSE=39.68). Sidik *et al.* (42) in their comparing two multicollinearity of PLSR and SMR methods, confirmed the prediction accuracy of SMR method was lower than PLSR method.

Table 4 Accuracy comparison of two different models (MLR and ANN)

	MLR	ANN
RMSEC (dS m^{-1})	9.331	2.410
RMSEV (dS m^{-1})	10.998	2.199
RMSE (dS m^{-1})	9.674	2.371
RSEC (dS m^{-1})	0.840	0.225
RSEV (dS m^{-1})	1.733	0.345
RSE (dS m^{-1})	0.949	0.240
MEC (dS m^{-1})	1.183	-0.067
MEV (dS m^{-1})	-0.789	-0.024
ME (dS m^{-1})	0.804	-0.059
R^2	0.506	0.964

Note: RMSEC and RMSEV are root mean square error in the calibration and validation processes respectively

According to Metternicht and Zinck (35) and Goldshleger *et al*. (25), salt causes variations in the surface roughness, which induces variation in the soil spectral reflectance. It means that many spectral properties such as the presence of salt crust, soil color and moisture content have a combined effect on saline soil reflectance. Thus, it is clear that using methods with applying combinations of spectral bands yield a better result than the actual band used for modeling and mapping soil salinity alone (36,54,45). The simplicity and fast optimization of MLR and ANN methods and acceptable degree of accuracy make them promising tools for use in soil salinity prediction.

5. Conclusion

We attempted to compare the linear and non-linear statistical prediction models of MLR and ANN in mapping soil salinity in a part of northeast of Iran. Although the performance of both methods were reliable in monitoring and predicting soil salinity, due to relatively high correlation between dependent variables and weak correlation between dependent and independent variables, the acquired coefficient of determination (R^2) of MLR prediction model was moderate (0.506). To overcome this slightly bad result, we propose that some terrain indices along with spectral indices can reveal a more efficient and reliable predicted soil salinity map in the same or larger scale than the present study area. The ANN predictive method was found to be more reasonable in predicting soil salinity with higher R^2 and lower error criteria in comparison with MLR model. It is suggested that other soil salinity prediction models, such as PLSR (partial least squares regression), should be applied in the study area to reduce the dimensions of independent variables in order to create more accurate spatial distribution map of soil affected areas.

Conflict of Interest

Despite efforts and researches to determine, monitor and reduce soil salinity in the study area, some villagers make conflicts unlike the projects by deviating irrigation canals toward their farmlands and it may lead to different results from the predictable ones.

Acknowledgment

In performing this research, Mr. Kazemnejad and Mr. Ghezel, staff of water and soil research office, Gorgan Department, had good cooperation. Their efforts are sincerely appreciated. The authors want to thank the anonymous reviewers for their invaluable

comments that led to a much improved manuscript.

Authors' Contributions

This research is a part of Phd. Thesis and professor Habibnejad and dr. Kavyan as the supervisors, Have significant contributions in development of the project. Also, this research have been improved in remote sensing and pedology with guidance of professor Solaimani and dr. Khormali as advisors.

Funding/Suppor

The authors need to thank the transportation of Kiakola municipality on their efforts on transporting to the region and supplying work forces.

References

1. Akhtar A, Shahbaz Kh, Nisar H, Munir AH, Suad A. Characterizing soil salinity in irrigated agriculture using a remote sensing approach, Phys Chem Earth. 2013; 1-10.
2. Akramkhanov A, Vlek PLG. The assessment of spatial distribution of soil salinity risk using neural network. Environ Monit Assess. 2012; 184: 2475-2485.
3. Allbed A, Kumar L, Sinha P. Mapping and Modelling Spatial Variation in Soil Salinity in the Al Hassa Oasis Based on Remote Sensing Indicators and Regression Techniques. J. Remote Sens. 2014; 6: 1137-1157.
4. Amini M, Afyuni M, Fathianpourb N, Khademi H, Fluchler H. Continuous soil pollution mapping usingfuzzy logic and spatial interpolation. Geoderma. 2005; 124: 223-233.
5. Aquastat. FAO's Information System onWater and Agriculture. 2016 [WWWDocument].
6. Asfaw E, Suryabhagavan KV, Argaw M. Soil salinity modeling and mapping using remote sensing and GIS: the case of Wenjisuger cane irrigation farm, Ethiopia. J Saudi Soc Agricul Sci. 2016; Accepted Manuscript.
7. Baret F, Guyot G. Potentials and limits of vegetation induces for LAI and APAR assessment. Remote Sens Environ. 1991; 535: 161-173.
8. Bierwirth PN, Brodie RS. Gama-ray remote sensing of Aeolian salt sources in the Murray-Darling Basin, Australia. Remote Sens. Environ. 2008; 112: 550-559.
9. Bihamta MR, Zare-Chahouki A. Principales of statistics for the natural resources science. Tehran: Tehran University; 2008. (In persian).
10. Buaziz M, Matschullat J, Gloaguen R. Improve remote sensing detection of soil salinity from a semi-arid climate in northeast Brazil. C.R. Geosci. 2011; 343: 795-803.
11. Cai S, Zhang R, Liu L, Zhou DA. Method of salt-affected soil informationextraction based on a support vector machine with texture features. Math Comput Model. 2010; 51 (11-12): 1319-1325.
12. Chang YM, Chang LC, Chang FJ. Comparison of static feedforward and dynamic-feedback neural networks for rainfall runoff modeling. J Hydro. 2004; 290: 297-311.
13. Chuangye S, Hangxu R, Chong H. Estimating soil salinity in the Yellow River Delta, eastern China-An integrated approach using spectral and terrain indices with the Generalized Additive Model Pedosphere. 2016; 26 (5): 626-635.
14. Clevers JGPW. The derivation of a simplified reflectance model for the

estimation of leaf area index. Remote Sens Environ. 1988; 25 (1): 53-70.

15. Clevers JGPW. The application of a weighted infrared vegetation index for estimating leaf area index by correcting soil moisture. Remote Sens Environ. 1989; 29: 23-37.

16. Colombani N, Mastrocicco M, Giambastiani BMS. Predicting salinization trends in a lowland coastal aquifer: Comacchio (Italy). Water Resour Manag. 2015; 29: 603-618.

17. Daliakopoulos IN,Tsanis IK, Koutroulis A, Kourglalas NN, Varouchakis AE, The threat of soil salinity: A European scale review. Sci Total Environ. 2016; 573: 727-739.

18. Demuth H, BealeM. Neural Network Toolbox for use with MatLab.User's guide version 4. 2004. The Math Works, Inc. 3 Apple Hill Drive, Natick, MA 01760-2098.

19. Douaoui AEK, Nicolas H, Walteer Ch. Detecting salinity hazards within a semiarid context by means of combining soil and remote sensing data. Geoderma. 2006; 134: 217-230.

20. Draper NR, Smith H. Applied Regression Analysis, third ed. New York: John Wiley & Sons, INC; 1998.

21. Farifteh J, Farshad A, George RJ, Assessing salt-affected soils using remotesensing, solute modelling, and geophysics. Geoderma. 2006; 130 (3-4): 191-206.

22. Farifteh J, Vander MF, Atzberger C, Carranza EJM. Quantitative analysis of salt-affected soil reflectance spectra: a comparison of two adaptivemethods (PLSR and ANN). Remote Sens Environ. 2007; 110 (1): 59-78.

23. Fernandez-Buces N, Siebe C, Cram S, Palacio JL. Mapping soil salinityusing a combined spectral response index for bare soil and vegetation: a casestudy in the former lake Texcoco, Mexico J Arid Environ. 2006; 65 (4):644-667.

24. Ghassemi F, Jakeman AJ, Nix HA. Salinization of Land and Water Resources: Human Causes, Extent, Management and Case Studies. The Australian National University/CAB International, Canberra, Australia/Wallingford, Oxon, UK. 1995.

25. Goldshleger N, Chudnovsky A, Ben-BinyaminR. Predicting salinity in tomato using soil reflectance spectral. Int J Remote Sens. 2013; 34: 6079-6093.

26. Gorji T, Sertel E, Tanik A. Manitoring soil salinity via remote sensing technology under data scarce conditions: a case study from Torkey. Ecol Indicators. 2017; 74: 384-391.

27. Haykin S. Neural networks: A comprehensive foundation. 2nd ed. New Jersey: Prentice–Hall Inc. 1999.

28. Huete AR, Jackson RD, Post DF. Spectral response of a plant canopy with different soil backgrounds. Remote Sens Environ. 1985; 17: 37-53.

29. Irons JR, Dwyer JL, Barsi JA. The next Landsat satellite: The Landsat Data Continuity Mission. Remote Sens Environ. 2012; 122: 11-21.

30. JafariHaghighi M. Methods for soil analysis. Tehran: NedayeZoha; 2003. (In Persian).

31. Khan NM, Rastoskuev VV, Shalina E, Sato Y. Mapping salt-affected soil using remote sensing indicators, A simple approach with the use of GIS Idrisi. 22nd Asian Conference on Remote Sensing, 5-9 November 2001, Singapore.

32. LiD J, Man-chun W, Tivip T. Study on soil salinization information in arid region using

remote sensing technique. Agr Sci China. 2011; 10 (3): 404-411.

33. Li S, Chen X. A new bare-soil index for rapid mapping developing areas using landsat8 data. The International Archives of the Photogrammetry, Remote Sens. Spatial Inform. Sci. volume XL-4. ISPRS Technical Commission IV Symposium, Suzhou, China This contribution. 14- 16 May 2014.

34. Metternicht GI. Categorical fuzziness: a comparison between crisp and fuzzyclassboundarymodelling for mapping salt-affected soils using Landsat TM data and a classification based on anion ratios. Ecol Model. 2003; 168 (3): 371-389.

35. Metternicht GI, Zinck JA. Remote sensing of soil salinity: potentials and constraints. Remote Sens Environ. 2003; 85: 1-20.

36. Noroozi AA, Homaee M, Farshad A. Integrated application of remote sensing andspatial statistical models to the identification of soil salinity: a case study fromGarmsarPlain, Iran J Environ Sci. 2012; 9: 59-74.

37. Qu YH, Duan XL, Gao HY, Chen AP, An YQ, Song JL, Zhou HM, He T. Quantitative retrieval of soil salinity using hyperspectral data in the region ofInner Mongolia Hetao irrigation district. Spectrosc Spect Anal. 2009; 29(5):1362-1366.

38. Rengasamy P. World salinization with emphasis on Australia. J Exp Bot. 2006; 57: 1017-1023.

39. Richardson AJ, Wiegand CL. Distinguishing vegetation from soil background information. Eng Remote Sens. 1997; 43: 1541-1542.

40. Rouse JW, Haas RH, Schelle JA, Deering DW, Harlan JC. Monitoring the vernal advancement or retro gradation of natural vegetation. NASA/GSFC, Type III, Final report, Green-belt, MD. 1974; p. 371.

41. Shoshany M, Goldshleger N,Chudnovsky A. Monitoring of agricultural soil degradation by remote-sensing methods: A review. Int J Remote Sens. 2013; 34(17): 6152-6181.

42. Sidik A, Zhao Sh, Wen Y. Estimating soil salinity in pingluo county of China using QuickBird data and soil reflectance spectra. Int J Appl Observ Geoinform. 2014; 26: 156-175.

43. Soil and water research Institute, Study improvement of irrigation, drainage and agricultural development for Gorgan plain, Golestan Province in Iran. Gorgan; 2003.

44. Taghizadeh-Mehrjardi R, Minasny B, Sarmadian F, Malone BP, Digital soil mapping of soil salinity in Ardakan region, central Iran. Geoderma. 2014; 213: 15-28.

45. Taghizadeh-Mehrjardi R, Sarmadian F, Savaghebi Gh, Omid M, Toomanian N, Roosta MJ, Rahimian MH. Comparison of Neuro-fazzy, ANFIS, ANN and MLR models in soil salinity prediction (case study: Ardakan City). J Nat Res Iran. 2013; 66(2): 207-222. (In Persian).

46. Tajgardan T, Ayoubi Sh, Shataii Sh, Khormali F. Mapping soil surface salinity using remote sensing data of ETM+ (Case study: North of AghGhala, Golestan Province). Water Soil Conserv. 2009; 16 (2): 1-17. (In Persian).

47. Tomasella J, Hodnett MG, Rossato L. Pedotransfer functions for the estimation of soil water retention in Brazilian soils. J Soil Sci Soc AM. 2000; 49: 1100-1105.

48. Urquhart EA, Zaitchik BF, Hoffiman MJ, Guikema, SD, Geiger EF. Remotely sensed estimates of surface salinity in the

Chesapeake Bay: a statistical approach. Remote Sens Environ. 2012; 123: 522-531.

49. Van Beek CL, TóthG. (Eds.), Risk Assessment Methodologies of Soil Threats in Europe, JRC Scientific and Policy Reports EUR. Luxembourg. Office for Official Publication of the European Communities 2012.

50. Weng YL, Gong P, Zhu ZL. A spectral indexfor estimating soil salinity in the Yellow River Delta Regionof China using EO-1 Hyperion data. Pedosphere. 2010; 20:378-388.

51. Wijaya A, Liesenberg V, Gloaguen R. Retrieval of forest attributesin complex successional forests of Central Indonesia: Modeling andestimation of bitemporal data. Forest Ecol Manag. 2010; 259(12): 2315-2326.

52. Wilding LP. Spatial variability: Its documentation, accommodation, and implication to soil survey. In: Nielsen, D.R., and J. Bouma, (eds.), Soil Spatial Variability, Pudoc, Wagenigen, the Netherlands. 1985; 166-194.

53. Yu R, Liu T, xu Y, Zhu C, Zhang Q, Quz. Analysis of salinization dynamics by remote sensing in Hetao Irrigation District of North China. agr. water manag. 2010; 97: 1952-1960.

54. Zewdu Sh, Suryabhagavan KV, Balakrishnan M. Land-use/Land-coverDynamics in Sego Irrigation Farm South Ethiopia Using Geospatial Tools. J Saudi Soc Agr Sci. 2016; 15: 91-97.

تهیه نقشه شوری خاک سطحی با استفاده از شاخص‌های دورسنجی در دشت آق قلا، ایران

سیده زهره موسوی[1*]، محمود حبیب نژاد[2]عطاالله کاویان[3]، کریم سلیمانی[2]، فرهاد خرمالی[4]

۱- دانشجوی دکتری آبخیزداری دانشکده منابع طبیعی، دانشگاه علوم کشاورزی و منابع طبیعی ساری، ساری، ایران
۲- استاد گروه آبخیزداری، دانشکده منابع طبیعی، دانشگاه علوم کشاورزی و منابع طبیعی ساری، ساری، ایران
۳- دانشیارگروه آبخیزداری، دانشکده منابع طبیعی، دانشگاه علوم کشاورزی و منابع طبیعی ساری، ساری، ایران
۴- استاد گروه خاکشناسی، دانشکده مهندسی آب و خاک، دانشگاه علوم کشاورزی و منابع طبیعی گرگان، گرگان، ایران

تاریخ دریافت: ۱۴ آبان ۱۳۹۵ / تاریخ پذیرش: ۲۰ اسفند ۱۳۹۵ / تاریخ چاپ: ۴ تیر ۱۳۹۶

مقدمه: شور شدگی خاک یک فرایند فروسایی اراضی با گسترش جهانی است که در مناطق خشک و نیمه خشک منجر به عواقب شدید اقتصادی و اجتماعی می‌شود.

مواد و روش‌ها: ما در این تحقیق شوری خاک را به دو روش آماری خطی (رگرسیون خطی چندگانه) و غیر خطی (شبکه عصب مصنوعی) و با استفاده از داده‌های ماهواره لندست، سنجنده OLI در دشت آق قلا واقع در شمال شرق ایران بررسی کرده‌ایم. هم‌چنین هدایت الکتریکی ۱۵۶ نمونه خاک سطحی برداشت شده از محل (عمق ۰-۱۵ سانتی‌متر) اندازه‌گیری شد. همیستگی پیرسون بین ۲۶شاخص طیفی به دست آمده از داده‌های لندست سنجنده OLI و ECهای اندازه‌گیری شده در محل انجام شد تا شاخص‌های کارآمد در شوری خاک بررسی شوند. وابسته‌ترین شاخص‌ها مثل باندهای آبی، سبز و قرمز، شاخص‌های شدت (Int1, Int2)، شاخص‌های شوری خاک (Aster-Si,Si1,Si2,Si3,Si11)، شاخص‌های گیاهی (NDVIDVI,RVI, SAVI) و شاخص‌های سبزینگی (Greenness) و رطوبت (Wetness) به عنوان متغیرهای مستقل برای گسترش دو مدل مورد استفاده قرار گرفتند.

نتایج: نتایج مقایسه دو مدل نشان داد که عملکرد مدل پیشگویی شبکه عصب مصنوعی (R^2=۰/۹۶۴ و RMSE=۲/۳۷۱) بهتر از عملکرد مدل رگرسیون خطی چندگانه (R^2=۰/۵۰۶ و RMSE=۹/۶۷۴) در نظارت و پیش‌بینی شوری خاک بوده است. از کل مساحت، ۶۶٪ و ۵۵/۸٪ به عنوان مناطق بدون شوری، با شوری کم و خیلی کم برای مدل‌های شبکه عصب مصنوعی و رگرسیون چند متغیره شناسایی شدند.

نتیجه‌گیری: این نشان می‌دهد که داده‌های سنجش از دور می‌توانند به طور موثری برای مدل‌سازی و تهیه نقشه شوری خاک در مناطق آبیاری مورد استفاده قرار گیرند.

کلمات کلیدی: ایران، داده‌های لندست OLI، رگرسیون خطی چندگانه، شبکه عصب مصنوعی، هدایت الکتریکی